Chapter 2

BASIC CONCEPTS

Ye (Geoffrey) Li

In this chapter, we first introduce the basic concepts of *orthogonal frequency division multiplexing* (OFDM), discuss the advantages and disadvantages compared single-carrier modulation, and present an implementation example. We then address various impairments of wireless channels on OFDM systems. Finally, we briefly describe other forms of multicarrier modulation.

2.1 Basic OFDM

High data-rate is desired in many applications. However, as the symbol duration reduces with the increase of data-rate, the systems using single-carrier modulation suffer from more severe *intersymbol interference* (ISI) caused by the dispersive fading of wireless channels, thereby needing more complex equalization. OFDM modulation divides the entire frequency selective fading channel into many narrow band flat fading subchannels[1] in which high-bit-rate data are transmitted in parallel and do not undergo ISI due to the long symbol duration. Therefore, OFDM modulation has been chosen for many standards, including *Digital Audio Broadcasting* (DAB) and terrestrial TV in Europe, and *wireless local area network* (WLAN). Moreover, it is also an important technique for high data-rate transmission over mobile wireless channels. Here we introduce the basic concepts of OFDM.

2.1.1 OFDM

OFDM was first introduced in [3], which is the form used in all present standards. It can be regarded as a time-limited form of multicarrier modulation.

Let $\{s_k\}_{k=0}^{N-1}$ be the complex symbols to be transmitted by OFDM mod-

[1]Subchannel is sometimes also called subcarrier or tone.

ulation; the OFDM (modulated) signal can be expressed as

$$s(t) = \sum_{k=0}^{N-1} s_k e^{\jmath 2\pi f_k t} = \sum_{k=0}^{N-1} s_k \varphi_k(t), \quad \text{for } 0 \le t \le T_s, \tag{2.1.1}$$

where $f_k = f_o + k\Delta f$ and

$$\varphi_k(t) = \begin{cases} e^{\jmath 2\pi f_k t} & \text{if } 0 \le t \le T_s, \\ 0 & \text{otherwise,} \end{cases} \tag{2.1.2}$$

for $k = 0,\ 1, \cdots, N-1$. T_s and Δf are called the *symbol duration* and *subchannel space* of OFDM, respectively. In order for receiver to demodulate OFDM signal, the symbol duration must be long enough such that $T_s \Delta f = 1$, which is also called *orthogonality condition.*

Because of the orthogonality condition, we have

$$\begin{aligned} & \frac{1}{T_s} \int_0^{T_s} \varphi_k(t) \varphi_l^*(t) dt \\ = & \frac{1}{T_s} \int_0^{T_s} e^{\jmath 2\pi (f_k - f_l)t} dt \\ = & \frac{1}{T_s} \int_0^{T_s} e^{\jmath 2\pi (k-l)\Delta f t} dt \\ = & \delta[k-l], \end{aligned} \tag{2.1.3}$$

where $\delta[k-l]$ is the delta function defined as

$$\delta[n] = \begin{cases} 1, & \text{if } n = 0, \\ 0, & \text{otherwise,} \end{cases}$$

Equation (2.1.3) shows that $\{\varphi_k(t)\}_{k=0}^{N-1}$ is a set of orthogonal functions. Using this property, the OFDM signal can be demodulated by

$$\begin{aligned} & \frac{1}{T_s} \int_0^{T_s} s(t) e^{-\jmath 2\pi f_k t} dt \\ = & \frac{1}{T_s} \int_0^{T_s} \left(\sum_{l=0}^{N-1} s_l \varphi_l(t) \right) \varphi_k^*(t) dt \\ = & \sum_{l=0}^{N-1} s_l \delta[l-k] \\ = & s_k. \end{aligned} \tag{2.1.4}$$

2.1.2 FFT Implementation

From (2.1.4), an integral is used for demodulation of OFDM signals. Here we describe the relationship between OFDM and *discrete Fourier transform* (DFT), which can be implemented by low complexity *fast Fourier transform* (FFT), as briefly indicated in Section 1.4.1.

From the previous discussion, an OFDM signal can be expressed as

$$s(t) = \sum_{k=0}^{N-1} s_k e^{j2\pi f_k t}.$$

If $s(t)$ is sampled at an interval of $T_{sa} = \frac{T_s}{N}$, then

$$S_n = s(n\Delta_s) = \sum_{k=0}^{N-1} s_k e^{j2\pi f_k \frac{nT_s}{N}}. \tag{2.1.5}$$

Without loss of generality, setting $f_o = 0$, then $f_k T_s = k$ and (2.1.5) becomes

$$S_n = \sum_{k=0}^{N-1} s_k e^{j\frac{2\pi kn}{N}} = \text{IDFT}\{s_k\},$$

where IDFT denotes the *inverse discrete Fourier transform*. Therefore, the OFDM transmitter can be implemented using the IDFT. For the same reason, the receiver can be also implemented using DFT.

The FFT algorithm provides an efficient way to implement the DFT and the IDFT. It reduces the number of complex multiplications from N^2 to $\frac{N}{2}\log_2 N$ for an N-point DFT or IDFT. Hence, with the help of the FFT algorithm, the implementation of OFDM is very simple, as shown in Figures 1.3 and 1.4.

2.1.3 Cyclic Extension, Power Spectrum, and Efficiency

To deal with delay spread of wireless channels, a cyclic extension is usually used in OFDM systems. There are three different types of cyclic extensions, which are shown in Figure 2.1. Denote T_g the length of a cyclic extension that is inserted between OFDM blocks. From Fig. 2.1 (b), OFDM signal, $s(t)$, can be extended into $\bar{s}(t)$ by

$$\bar{s}(t) = \begin{cases} s(t), & \text{if } 0 \le t \le T_s, \\ s(t - T_s), & \text{if } T_s < t \le T_s + T_g (= T). \end{cases} \tag{2.1.6}$$

With the cyclic extension, the actual OFDM symbol duration is increased from T_s to $T = T_s + T_g$. In the following discussion, the cyclic suffix extension in Fig. 2.1 (b) is assumed. However, the results can be also applied to the other types of cyclic extension.

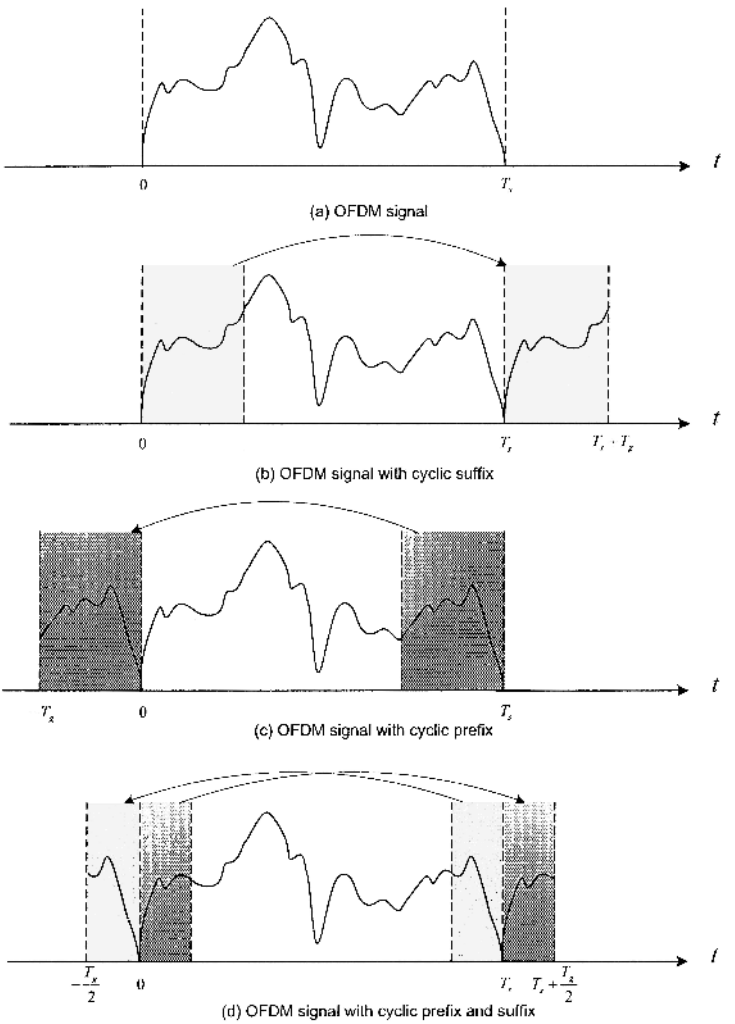

Figure 2.1. OFDM signal with different cyclic extensions.

Because $s(t)$ in (2.1.1) is a summation of truncated complex exponential functions with different frequencies, the power density spectrum of $s(t)$ consists of $|\sin(f)/f|^2$-shaped spectra, as sketched in Fig. 2.2.

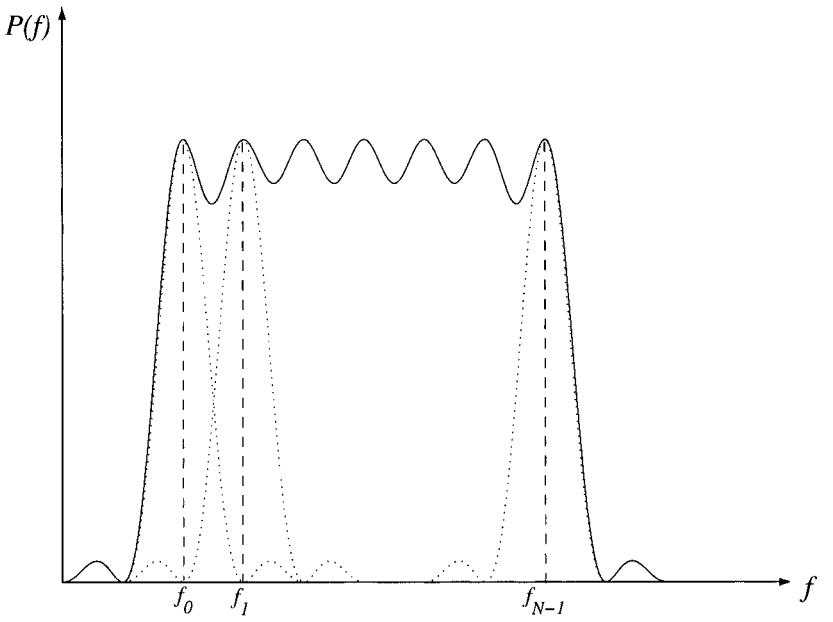

Figure 2.2. Power spectrum of OFDM Signal.

Fig. 2.2 shows that, for an OFDM signal consisting of N subchannels, the signal bandwidth is about $(N+1)\Delta f$. Since the transmission rate of each subchannel is $\frac{1}{T}$ symbols/sec., the *total transmission rate* of OFDM signal is $\frac{N}{T}$ symbol/sec. Therefore, the bandwidth efficiency of the OFDM system is

$$\begin{aligned} \eta &= \frac{N/T}{(N+1)\Delta f} \\ &= \frac{N/(T_s+T_g)}{(N+1)/T_s} \\ &= \frac{1}{1+\frac{1}{N}} \frac{1}{1+\frac{T_g}{T_s}}, \end{aligned} \tag{2.1.7}$$

in symbols/sec/Hz. For most practical OFDM systems, N is much larger than 1 and the guard interval or cyclic extension is much smaller than the

OFDM symbol duration, so $W \approx 1$. If each symbol carries k bit information, the bandwidth efficiency will be k bits/sec/Hz.

2.1.4 Comparison with Single-Carrier

As indicated in [33], the dispersive Rayleigh fading in wireless channels limits the highest data rate of single-carrier systems. To reduce the effect of ISI in unequalized systems, the symbol duration must be much larger than the delay spread of wireless channels. In OFDM, the entire channel is divided into many narrow subchannels, which are transmitted in parallel, thereby increasing the symbol duration and reducing the ISI. Therefore, OFDM is an effective technique for combating multipath fading and for high-bit-rate transmission over mobile wireless channels.

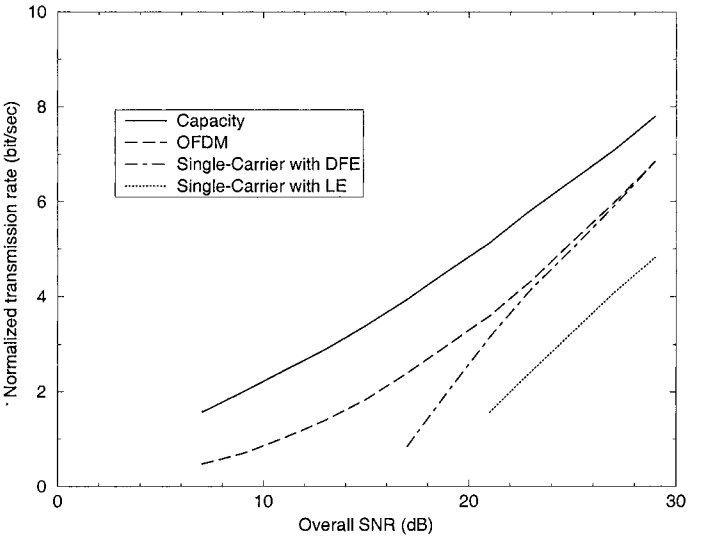

Figure 2.3. Transmission rate of OFDM and single-carrier systems for AWGN channel.

Figure 2.3, from [23], compares the transmission rate of an OFDM system with that of a single-carrier system using a *decision-feedback equalizer* (DFE)

or a *linear equalizer* (LE). Note that the curve for the DFE in the figure is obtained by assuming that the feedback symbols at the DFE are error free, so it is in fact an upper bound for the transmission rate of the DFE. From the figure, for the same overall SNR, the normalized transmission rate of the OFDM system is much higher than that of the single-carrier system.

2.1.5 Design Example

Here, we present a simple example to demonstrate the design of an OFDM system. Consider a sample system that is required to transmit 1.2 Mbits/sec using *quadrature PSK* (QPSK) over an 800 kHz bandwidth in a wireless environment with a maximum delay span up to 40 μsec. Note that from the results in [33], for a channel with a 40-μsec delay span, the maximum symbol rate is only 5 kbaud. It is obvious that the required transmit rate can not be obtained by a single-carrier system. However, it can be easily achieved using OFDM modulation.

To construct the OFDM signal, we assume the entire channel bandwidth, 800 kHz, is divided into N=128 subchannels or tones. Thus, the subchannel or subchannel space is 6.25 kHz. Let the 4 subchannels on each end be used as guard tones to facilitate filtering, and the rest (120 tones) are used to transmit data. To make the tones orthogonal to each other, the symbol duration is $T_s = 160$ μsec. An additional $T_g = 40$ μsec cyclic extension is used to provide protection from intersymbol interference due to channel multipath delay spread. This results in a total block length $T = 200$ μsec and a subchannel symbol rate $r_b = 5$ kbaud. For QPSK, each symbol carries 2 bit information; consequently, the data transmission rate of the OFDM system is

$$R_b = \frac{120 \times 2 \text{ bits}}{200 \ \mu\text{sec}} = 1.2 \text{ Mbits/sec}.$$

2.1.6 Baseband versus Passband

In Sections 2.1.1-2.1.5, the OFDM signals are complex baseband signals. However, in wireless communication systems, *complex* baseband signals must be converted into *real* passband signals. In this section, we briefly introduce the baseband and passband representations.

The baseband signal, $s(t)$, is usually a complex function of time. Therefore, it can be written into rectangular form as

$$s(t) = s_I(t) + js_Q(t),$$

where the real part, $s_I(t)$, is called *in-phase component* of the baseband signal; and the imaginary part, $s_Q(t)$, is called *quadrature component.* For the baseband OFDM signal in (2.1.1), we have

$$\begin{aligned} s(t) &= \sum_{k=0}^{N-1} (\Re\{s_k\}\cos(2\pi f_k t) - \Im\{s_k\}\sin(2\pi f_k t)) \\ &\quad + \jmath \sum_{k=0}^{N-1} (\Im\{s_k\}\cos(2\pi f_k t) + \Re\{s_k\}\sin(2\pi f_k t)), \end{aligned}$$

and therefore,

$$s_I(t) = \sum_{k=0}^{N-1} (\Re\{s_k\}\cos(2\pi f_k t) - \Im\{s_k\}\sin(2\pi f_k t)),$$

and

$$s_Q = \sum_{k=0}^{N-1} (\Im\{s_k\}\cos(2\pi f_k t) + \Re\{s_k\}\sin(2\pi f_k t)),$$

where $\Re\{s_k\}$ and $\Im\{s_k\}$ denote the real and imaginary parts of the complex symbol s_k, respectively.

Figure 2.4 shows conversion between baseband and passband signals. From the figure, the passband signal can be expressed as

$$\begin{aligned} s_p(t) &= \Re\{s(t)e^{\jmath 2\pi f_c t}\} \\ &= s_I(t)\cos(2\pi f_c t) - s_Q(t)\sin(2\pi f_c t), \end{aligned}$$

where f_c is the carrier frequency of a communication system. It is assumed that the variations of the signal are much slower than the carrier frequency. For OFDM, the passband signal can be further simplified as

$$\begin{aligned} s_p(t) &= s_I(t)\cos(2\pi f_c t) - s_Q(t)\sin(2\pi f_c t) \\ &= \sum_{k=0}^{N-1} (\Re\{s_k\}\cos(2\pi(f_c + f_k)t) - \Im\{s_k\}\sin(2\pi(f_c + f_k)t)). \end{aligned}$$

If we denote the magnitude and the phase of complex symbol, s_k, as d_k and θ_k, respectively, that is, $s_k = d_k e^{\jmath\theta_k}$, then

$$s_p(t) = \sum_{k=0}^{N-1} d_k \cos(2\pi(f_c + f_k)t + \theta_k).$$

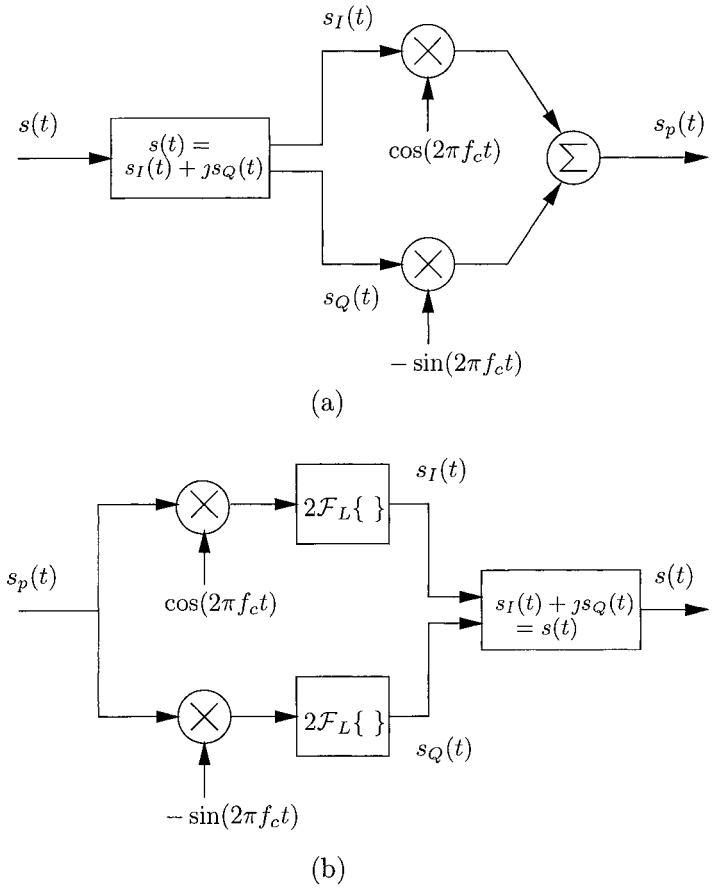

Figure 2.4. Baseband versus passband: (a) baseband to passband conversion, and (b) passband to baseband conversion.

At the receiver, the baseband signal can be obtained from the passband signal. Figure 2.4 (b) shows conversion from the baseband signal to the passband signal, where $\mathcal{F}_L$ represents a low-pass filter operation. From Fig. 2.4 (b), we have

$$\begin{aligned} s(t) &= 2\mathcal{F}_L\{s_p(t)\cos(2\pi f_c t) - js_p(t)\sin(2\pi f_c t)\} \\ &= 2\mathcal{F}_L\{s_p(t)e^{-j2\pi f_c t}\}. \end{aligned}$$

Similarly, the linear distortion of any physical channel can be also equivalent to a *baseband (complex) channel*, $h(t)$, so that the baseband channel output is the convolution of the baseband signal and the baseband channel impulse response, *i.e.*

$$x(t) = s(t) \circledast h(t) = \int_{-\infty}^{+\infty} s(\tau)h(t-\tau)d\tau.$$

More detailed information about baseband and passband conversion can be obtained from Proakis [34].

2.2 Impairments of Wireless Channels to OFDM Signals

In this section, we introduce the impairments in OFDM systems, including Doppler shift, dispersive fading, timing and frequency offsets, sampling clock offset, and nonlinear distortion due to large *peak-to-average-power ratio* (PAPR) of the OFDM signal.

2.2.1 Time-Varying Impairments

Both Doppler shift and frequency offset can be modelled as time-varying impairments. Here we first derive a general expression for the effect of the time-varying impairments and then discuss the effect of Doppler shift and frequency offset, respectively.

Consider an OFDM signal,

$$s(t) = \sum_k s_k e^{j2\pi f_k t}, \quad 0 \leq t \leq T_s,$$

where $f_k = f_o + k\Delta f$ and s_k is the signal transmitted over the k-th subchannel. If there is a multiplicative time-varying distortion, $\gamma(t)$, that is caused by either frequency offset or Doppler spread, the received signal will be

$$x(t) = \gamma(t)s(t). \tag{2.2.1}$$

The demodulated signal will be [2]

$$\begin{aligned} X_m &= \frac{1}{T_s}\int_0^{T_s} x(t)e^{-\jmath 2\pi f_m t}dt \\ &= \frac{1}{T_s}\int_0^{T_s} \gamma(t)\sum_k s_k e^{\jmath 2\pi f_k t}e^{-\jmath 2\pi f_m t}dt \\ &= \sum_k \left\{\frac{1}{T_s}\int_0^{T_s}\gamma(t)e^{-\jmath 2\pi(f_m-f_k)t}dt\right\} s_k \\ &= a_0 s_m + \underbrace{\sum_{k\neq m} a_{m-k}s_k}_{ICI}, \end{aligned} \tag{2.2.2}$$

where a_l is defined as

$$a_l \triangleq \frac{1}{T_s}\int_0^{T_s}\gamma(t)e^{-\jmath 2\pi l\Delta f t}dt. \tag{2.2.3}$$

a_0 is usually a complex number, whose magnitude and phase represent the attenuation and the phase shift on the desired signal, respectively. a_l's, for $l \neq 0$, are complex gains of the *interchannel interference* (ICI). If $\gamma(t)$ is not a constant, then $a_l \neq 0$ for some $l \neq 0$, and ICI exists.

Effect of Frequency Offset

If there is a frequency offset, δf, between the transmitter and the receiver, then $\gamma(t)$ in (2.2.1) is a deterministic function and can be expressed as

$$\gamma(t) = e^{\jmath 2\pi\delta f t} = e^{\jmath 2\pi\alpha\Delta f t},$$

where $\alpha = \frac{\delta f}{\Delta f}$. From (2.2.3), we have

$$\begin{aligned} a_l &= \frac{1}{T_s}\int_0^{T_s} e^{\jmath 2\pi\alpha\Delta f t}e^{-\jmath 2\pi l\Delta f t}dt \\ &= \frac{\sin[\pi(l-\alpha)]}{\pi(l-\alpha)}e^{-\jmath\pi(l-\alpha)} \\ &= -\frac{\sin(\pi\alpha)}{\pi(l-\alpha)}e^{\jmath\pi\alpha}. \end{aligned} \tag{2.2.4}$$

[2]For simplicity, an integral is used here instead of the DFT. However, the integration is almost the same as the DFT for systems with a large number of carriers.

Let $\alpha = k_o + \epsilon$, where k_o is an integer and ϵ is a fractional number with $|\epsilon| \leq 1/2$, then

$$a_l = -\frac{\sin(\pi\epsilon)}{\pi(l - k_o - \epsilon)} e^{+j\pi\epsilon}. \tag{2.2.5}$$

When $\alpha \leq 1/2$ ($k_o = 0$ and $\epsilon = \alpha$), $0 < |a_l| \leq |a_0|$. The desired signal is the dominant component in the demodulated signal. However, there is also ICI since $a_l \neq 0$ for $l \neq 0$. When α is an integer ($k_o = \alpha$ and $\epsilon = 0$), $a_{k_o} = 1$, $a_l = 0$ for $l \neq k_o$, and $X_l = s_{l-k_o}$. Therefore, the frequency offset causes a simple tone shift and there is no ICI. In general, neither k_o nor ϵ is zero; consequently, tone shift, attenuation, phase shift, and ICI all exist. However, the signal distortion caused by frequency offset is deterministic. Furthermore, once the frequency offset is known, its effect can be corrected. Chapter 4 will present techniques for frequency offset estimation and correction in OFDM systems, where coarse and fine synchronization is used to cancel the effects of k_o and ϵ, respectively.

Effects of Doppler Shift

For channels with Doppler spread, $\gamma(t)$ is can be modelled as a zero-mean and narrow-band *wide-sense stationary* (WSS) stochastic process. For the classical Doppler spectrum [35], the spectral density of $\gamma(t)$ is

$$P_J(f) = \begin{cases} \frac{1}{\pi f_d} \frac{1}{\sqrt{1-(\frac{f}{f_d})^2}}, & \text{if } |f| < f_d, \\ 0, & \text{otherwise,} \end{cases} \quad \text{(Classical)}$$

where f_d is the maximum Doppler frequency. Two extreme cases of the Doppler spectrum are the uniform and the two-path models, which have been studied in [36]. For these two models, the spectral densities are

$$P_u(f) = \begin{cases} \frac{1}{2f_d} & \text{if } |f| < f_d, \\ 0, & \text{otherwise,} \end{cases} \quad \text{(Uniform)}$$

and

$$P_t(f) = \frac{1}{2}[\delta(f + f_d) + \delta(f - f_d)], \quad \text{(Two-path)}$$

respectively. The correlation function of $\gamma(t)$, defined as $r(\tau) = E\{\gamma(t + \tau)\gamma^*(t)\}$, is easily obtained as

$$r(\tau) = \mathcal{F}^{-1}\{P(f)\}.$$

The correlation functions for the three models given above are

$$r_J(\tau) = J_0(2\pi f_d \tau), \quad \text{(Classical)}$$

$$r_u(\tau) = \text{sinc}(f_d \tau), \quad \text{(Uniform)}$$

and

$$r_t(\tau) = \cos(2\pi f_d \tau), \quad \text{(Two-path)}$$

respectively, where $J_0(x)$ is the zero-order Bessel function of the first kind and

$$\text{sinc}(x) \triangleq \frac{\sin(\pi x)}{\pi x}.$$

It should be noted that the two-path model corresponds to an OFDM system with a fixed frequency offset of f_d Hz.

Since $\gamma(t)$ is a stochastic process, from (2.2.3), a_l is a random variable. Furthermore, it is proved in [37] that a_l is zero mean and with variance

$$\sigma_l^2 \triangleq E\{|a_l|^2\} = \int_{-1}^{1} r(T_s x)(1 - |x|)e^{-\jmath 2\pi l x} dx,$$

and the total ICI power due to Doppler spread is

$$\begin{aligned} P_{ICI} &\triangleq E\left|\sum_{l \neq 0} a_l s_{m-l}\right|^2 \\ &= \int_{-1}^{1} (1 - |x|)\,(1 - r(T_s x))\, dx \\ &= 1 - \int_{-f_d}^{f_d} P(f)\text{sinc}^2(fT_s) df. \end{aligned} \tag{2.2.6}$$

Once the time-domain correlation or the Doppler spectral density of the time-varying channel is known, the ICI power can be calculated. For the classical model, we have

$$P_{ICI} = 1 - \int_{-1}^{1} (1 - |x|) J_0(2\pi f_d T_s x) dx, \tag{2.2.7}$$

which was first derived by Russell and Stüber [38]. For the uniform and two-path models, we have

$$P_{ICI} = 1 - \frac{1 - \cos(2\pi f_d T_s) - 2\pi f_d T_s \text{Si}(2 f_d T_s)}{2(\pi f_d T_s)^2}, \tag{2.2.8}$$

Table 2.1. α_1's and α_2's for different time-varying models

model	α_1	α_2
Classical	1/2	3/8
Uniform	1/3	1/5
Two-path	1	1

and

$$P_{ICI} = 1 - \text{sinc}^2(f_d T_s), \tag{2.2.9}$$

respectively, where

$$\text{Si}(x) = \pi \int_0^x \frac{\sin(\pi u)}{\pi u} du = \pi \int_0^x \text{sinc}(u) du.$$

The expressions in (2.2.8) and (2.2.9) were first derived by Robertson and Kaiser [36].

Using the expressions derived above, the ICI power can be exactly calculated. However, the exact expressions are complicated and do not easily provide much insight. Furthermore, in many instances, the exact time-domain correlation or power spectrum is not available. Here, we introduce several bounds on the ICI power, which are derived in [37]. These bounds are less complicated and the insight is more readily obtained.

It has been proved in [37] that the ICI power has the following lower and upper bounds:

$$P_{ICI} \geq \frac{\alpha_1}{12}(2\pi f_d T_s)^2 - \frac{\alpha_2}{360}(2\pi f_d T_s)^4, \tag{2.2.10}$$

and

$$P_{ICI} \leq \frac{\alpha_1}{12}(2\pi f_d T_s)^2, \tag{2.2.11}$$

where α_i's, for $i = 1, 2$, are defined as

$$\alpha_k \triangleq \frac{1}{f_d^{2k}} \int_{-f_d}^{f_d} f^{2k} P(f) df = \frac{2}{f_d^{2k}} \int_0^{f_d} f^{2k} P(f) df.$$

The constants α_1 and α_2 are easy to calculate and are given in Table 2.1 for the three models introduced before.

It should be indicated that without knowing the Doppler spectrum, α_1 and α_2 can be also evaluated using other approaches. For example, it can

be proved that

$$E\left\{\left|\gamma^{(k)}(t)\right|^2\right\} = (2\pi)^{2k}\int_{-f_d}^{f_d} f^{2k}P(f)df,$$

where $\gamma^{(k)}(t) = \frac{d^k\gamma(t)}{dt^k}$. Then, α_k can be evaluated by

$$\alpha_k = \frac{E\left\{\left|\gamma^{(k)}(t)\right|^2\right\}}{(2\pi f_d)^{2k}},$$

which is much simpler than obtaining by the Doppler spectrum.

From the definition of α_1, it is clear that $\alpha_1 \leq 1$. Using this fact, together with (2.2.11), we can obtain a *universal upper bound* on the ICI power, which depends only on f_dT_s,

$$P_{ICI} \leq \frac{1}{12}(2\pi f_dT_s)^2. \tag{2.2.12}$$

This universal upper bound can be used in OFDM systems with any Doppler spectra, including with frequency offset. Since α_1 is no more than 1, the above bound is looser than the bound in (2.2.11). However, (2.2.12) is much easier to calculate since it only depends on f_dT_s. For the two-path model, $\alpha_1 = 1$, and the universal bound is also the tight bound.

In the above discussions, we have introduced tight and universal bounds for time-varying flat fading channels. For OFDM systems with a proper cyclic extension, the exact expressions for the ICI power and the various bounds are also applicable to time-varying dispersive channels.

In Figure 2.5, we compare the upper and the lower tight bounds and the universal bound with the exact value of the ICI power for the classical Doppler spectrum. From Fig. 2.5, the tight bounds are very close to the exact ICI power. When designing OFDM systems, if symbol duration, T_s, is chosen so that f_dT_s is very small, then the ICI due to Doppler spread will be negligible. In the design example in Section 2.1.1, $T_s = 160$ μsec, then $P_{ICI} < 0.168\%$(-27.7 dB) when $f_d = 200$ Hz. Therefore, the P_{ICI} is much less than the noise or co-channel interference level.

Though Doppler shift has only minor effect on the ICI of OFDM signals when f_dT_s is very small. It *does* make the channel parameters to vary from one OFDM block to another. Therefore, when channel parameters are used for coherent detection or adaptive antenna arrays in mobile wireless systems, channel tracking is still essential in most environments. In Chapter 5, we describe different channel parameter estimation approaches.

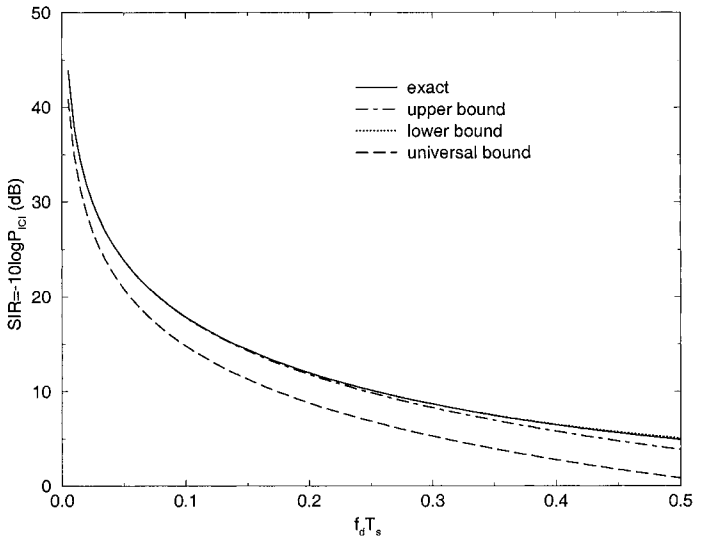

Figure 2.5. Comparison of exact P_{ICI}, its upper and lower bounds, and universal bound for the classical model.

2.2.2 Effect of Sampling Clock Offset

In practice, the sampling clock at the receiver is often different from that at the transmitter. The sampling clock difference will degrade the performance of the systems. As discussed in Section 2.1.2, OFDM signal can be simply demodulated by performing DFT to the samples if the continuous signal $s(t) = \sum_{k=0}^{N-1} s_k e^{j2\pi f_k t}$ is sampled at a sampling interval of $T_{sa} = \frac{T_s}{N}$ at the receiver. However, if the sampling interval at the receiver is $T'_{sa} = T_{sa} + \beta T_{sa}$, other than T_{sa}, then the samples will be $\{s(nT'_{sa})\}_{n=0}^{N-1}$. If DFT is still used

for OFDM demodulation [39], then we will have

$$\begin{aligned} X_m &= \frac{1}{N}\sum_{n=0}^{N-1} s(nT'_{sa})e^{-\jmath 2\pi\frac{nm}{N}} \\ &= a_{m,m}s_m + \sum_{k\neq m} a_{m,k}s_k, \end{aligned} \tag{2.2.13}$$

where

$$a_{m,k} = \frac{\sin[\pi(k-m+\beta k)]}{N\sin[\frac{\pi}{N}(k-m+\beta k)]}e^{\jmath\pi\frac{N-1}{N}(k-m+\beta k)}.$$

From (2.2.13), the demodulated signal, X_m, consists of the desired symbol component, s_m, and ICI. The desired symbol is modified by

$$\begin{aligned} a_{m,m} &= \frac{\sin(\pi\beta m)}{N\sin(\frac{\pi}{N}\beta m)}e^{\jmath\pi\frac{N-1}{N}\beta m} \\ &\approx e^{\jmath\pi\beta m}, \end{aligned}$$

which is a subchannel-dependent phase rotation. In the above approximation, we have assumed that $N \gg 1$ and $\beta N \ll 1$, which is usually true in practice. It can be also shown in [39] that the average ICI power at the m-th subchannel is

$$\begin{aligned} P_{ICI}[m] &= E\left|\sum_{k\neq m} a_{m,k}s_k\right|^2 \\ &\approx \frac{\pi^2}{3}\beta^2 m^2, \end{aligned}$$

which is also subchannel-dependent.

In Section 4.4, we will briefly discuss sampling clock offset estimation and correction.

2.2.3 Effect of Timing Offset

In Figure 2.6, the effect of timing offset on an OFDM signal is shown. When there is a timing offset, $\tau > 0$[3], between the transmitter and the receiver, the observed signal will be

$$\bar{s}(t,\tau) = \begin{cases} s(t+\tau), & \text{if } 0 \le t \le T_s - \tau, \\ e(t-T_s+\tau), & \text{if } T_s - \tau \le t \le T_s. \end{cases}$$

[3]Even through we assume that $\tau > 0$ here, the derived result can be also used to the case with $\tau < 0$

where $e(t)$ denotes interference due to the timing offset. For OFDM systems without a guard interval or cyclic extension, $e(t)$ is a part of next OFDM block, as shown in Fig. 2.6 (a). For OFDM systems with a guard interval larger than τ, $e(t) = 0$, as shown in Fig. 2.6 (b). For OFDM systems with a cyclic extension period larger than τ, $e(t) = s(t)$, as shown in Fig. 2.6 (c). For OFDM systems with a cyclic extension period or guard interval less than τ, $e(t)$ is a mixture of the above two or three signals.

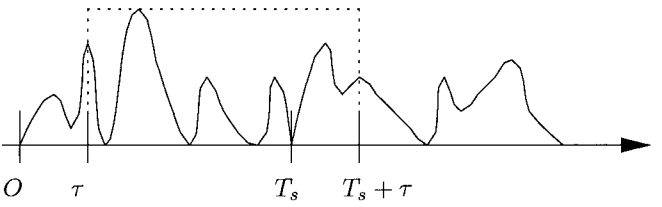

(a) $e(t)$ is a part of the next block

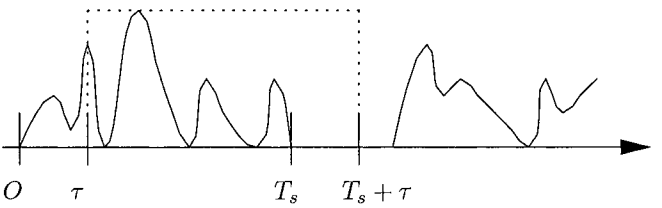

(b) $e(t)$ is a part of guard interval

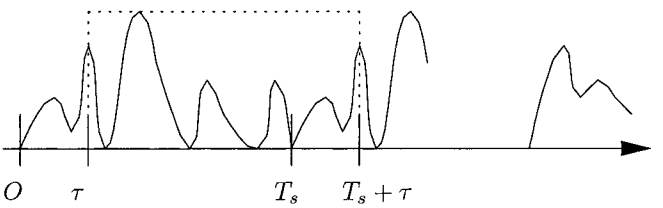

(c) $e(t)$ is a part of cyclic extension

Figure 2.6. Effect of timing offset on OFDM signal.

When there is a timing offset, the demodulated signal at the receiver is

$$\begin{aligned} X_m &= \frac{1}{T_s}\int_0^{T_s} \bar{s}(t,\tau)e^{-\jmath 2\pi f_m t}dt \\ &= \frac{1}{T_s}\int_0^{T_s-\tau} s(t+\tau)e^{-\jmath 2\pi f_m t}dt + \frac{1}{T_s}\int_{T_s-\tau}^{T_s} e(t-T_s+\tau)e^{-\jmath 2\pi f_m t}dt \\ &= \frac{1}{T_s}\int_{\tau}^{T_s} s(t)e^{-\jmath 2\pi f_m (t-\tau)}dt + \frac{1}{T_s}\int_0^{\tau} e(t)e^{-\jmath 2\pi f_m (t-\tau)}dt \\ &= \frac{1}{T_s}\int_0^{T_s} s(t)e^{-\jmath 2\pi f_m (t-\tau)}dt - \frac{1}{T_s}\int_0^{\tau} s(t)e^{-\jmath 2\pi f_m (t-\tau)}dt \\ &\quad + \frac{1}{T_s}\int_0^{\tau} e(t)e^{-\jmath 2\pi f_m (t-\tau)}dt \\ &= s_m e^{\jmath 2\pi f_m \tau} + \frac{1}{T_s}\int_0^{\tau} [e(t)-s(t)]e^{-\jmath 2\pi f_m (t-\tau)}dt. \end{aligned} \tag{2.2.14}$$

From (2.2.14), timing offset introduces a phase shift to the desired symbol component and an additive interferer depending on whether a cyclic extension or a null interval is used. When the system has no guard interval or cyclic extension, then as shown in Fig. 2.6, $e(t)$ is a part of the next OFDM block, which is independent of $s(t)$. Therefore, the resulting average interference power is the summation of the powers $\frac{1}{T_s}\int_0^{\tau} s(t)e^{\jmath 2\pi f_m (t-\tau)}dt$ and $\frac{1}{T_s}\int_0^{\tau} e(t)e^{\jmath 2\pi f_m (t-\tau)}dt$. When the system has a guard interval that is larger than τ, then $e(t) = 0$, only single term remains. However, if a proper cyclic extension is used as in Fig. 2.6 (c), then $e(t) = s(t)$ and there is no interference. Therefore, a proper cyclic extension can effectively cancel additive interference caused by timing offset.

In Chapter 4, timing offset estimation is introduced. With estimated timing offset, the sampling time and integration region can be adjusted to reduce the induced phase shift on the desired symbol and to mitigate additive interference.

2.2.4 Effect of Delay Spread

For a channel with multipath delay spread, the received signal is a summation of the transmitted signal with different (complex) gains and delays, as shown in Fig. 2.7. Here we assume that the transmitted signal has a proper cyclic suffix extension and the length of the cyclic extension, T_g, is larger than the delay span or channel length, T_h, of the multipath fading channel.

Furthermore, we assume that the starting time of integration/observation is between T_h and T_g, that is, $T_h \leq \tau \leq T_g$.

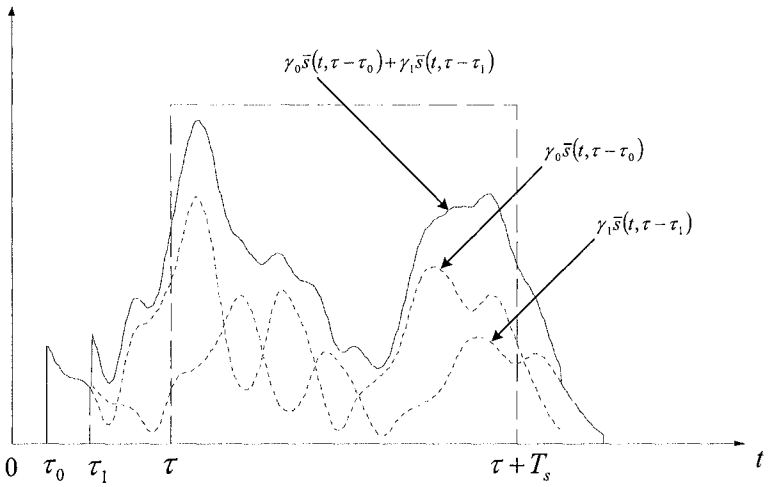

Figure 2.7. Effect of delay spread on OFDM signal.

Let the gain and delay of each path be γ_i and τ_i, respectively. As shown in Figure 2.7, the received signal can be expressed as

$$x(t) = \sum_i \gamma_i \bar{s}(t, \tau - \tau_i).$$

Therefore, the demodulated signal at the receiver is

$$\begin{aligned} X_m &= \frac{1}{T_s}\int_0^{T_s} r(t)e^{-j2\pi f_m t}dt \\ &= \sum_i \gamma_i \frac{1}{T_s}\int_0^{T_s} \bar{s}(t, \tau - \tau_i)e^{-j2\pi f_m t}dt. \end{aligned}$$

When $\tau_{max} \leq \tau \leq T_g$, from (2.2.14), we have

$$\frac{1}{T_s}\int_0^{T_s} \bar{s}(t, \tau - \tau_i)e^{-j2\pi f_m t}dt = s_m e^{j2\pi f_m(\tau-\tau_i)}.$$

Hence,

$$\begin{aligned} X_m &= \sum_i \gamma_i s_m e^{\jmath 2\pi f_m(\tau-\tau_i)} \\ &= s_m e^{\jmath 2\pi f_m \tau} \sum_i \gamma_i e^{-\jmath 2\pi f_m \tau_i} \\ &= H(f_m) e^{\jmath 2\pi f_m \tau} s_m, \end{aligned} \tag{2.2.15}$$

where $H(f)$ is the frequency response of the multipath channel defined as

$$H(f) = \sum_i \gamma_i e^{-\jmath 2\pi f \tau_i}.$$

From (2.2.15), the received symbol is the original symbol with a phase shift determined by the timing offset, and multiplicative distortion determined by the frequency response at each subchannel, which makes signal detection very simple and is also a crucial difference between OFDM and single-carrier modulation. For single-carrier modulation, delay spread or frequency selectivity of wireless channels will cause ISI, which makes signal detection very complicated.

In Chapters 4 and 5, we will introduce various timing offset estimation and channel estimation approaches, respectively. Once the timing offset and channel parameters are estimated, the phase shift and the multiplicative distortion can be corrected.

2.2.5 System Nonlinearity

Nonlinear devices in wireless systems will distort OFDM signals. In this section, we will briefly discuss the impact of system nonlinearity on OFDM signals.

In Chapter 1.6, the PAPR of OFDM signals has been discussed. It can be easily checked that for an OFDM signal with N subchannels the peak power can be as large as N^2 while the average power is N when $\mathrm{E}\{|s_k|^2\} = 1$; consequently, the largest PAPR will be

$$\text{PAPR} = N.$$

For an OFDM signal with 128 subchannels, PAPR=21 dB, while it is about 6 dB for single carrier modulation. It should be noted that the probability for an OFDM signal to have a large PAPR is very small even though the largest possible PAPR is very large.

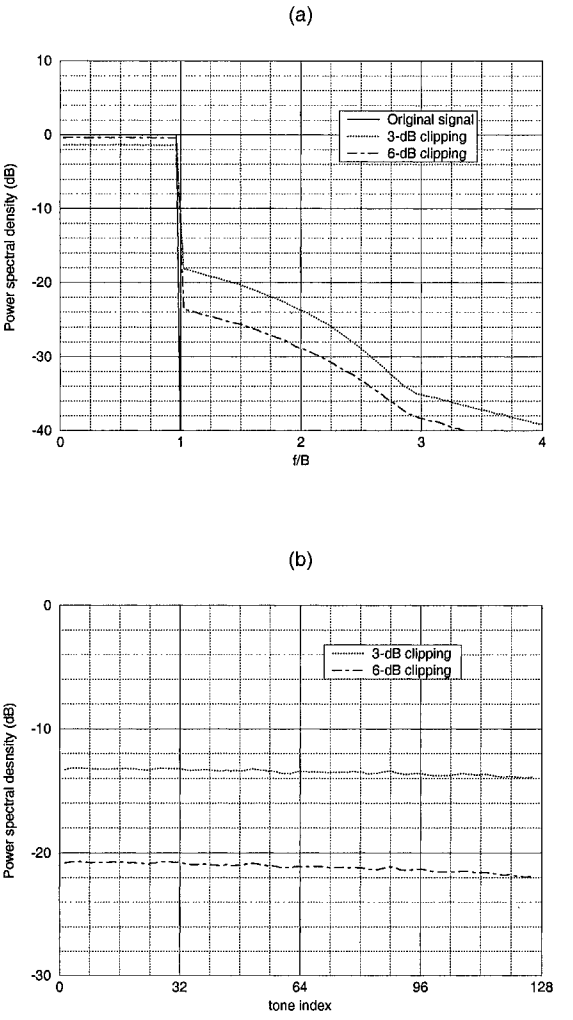

Figure 2.8. (a) Spectral spread and (b) inband distortion caused by clipping.

When an OFDM signal is passed through a nonlinear device, such as a transmitter power amplifier, it will suffer significant nonlinear distortion, which generates spectral spreading and in-band noise. Figure 2.8 demon-

strates inband distortion and spectral spread due to the nonlinearity of an amplifier. If the amplifier is modeled as a 3-dB clipper, then it will cause about 14 dB inband noise, about 22 dB adjacent channel interference. As indicated in [40], adjacent channel interference or spectral spread can be mitigated by a clipping-and-filtering algorithm. However, inband noise still degrades the system performance. In Chapter 6, we will present different PAPR reduction techniques for OFDM systems.

2.3 Other Multicarrier Modulation

In the previous sections, we have introduced OFDM modulation, which belongs to a more general group of multicarrier modulation,. In this section, we briefly present two band-limited multicarrier approaches: orthogonal and filter modulation.

2.3.1 Orthogonal Approach

The orthogonal approach was proposed by Chang in [9]. It is shown in Figure 2.9, where $s_{n,k}$ and $X_{n,k}$ are the transmitted and demodulated symbols, respectively, at the k-th subchannel of the n-th OFDM block. The filters in the figure are band-limited and with overlap in the frequency domain. Therefore, their frequency responses must satisfy certain conditions so that the transmitted signal can be demodulated at the receiver.

Denote $\Phi_k(f) = |\Phi_k(f)| \exp\{j\theta_k(f)\}$ the frequency response of the k-th filter in Fig. 2.9. The receiver can recover the transmitted signal without any ISI and ICI at the receiver if the amplitude and the phase of the frequency response satisfy the following conditions [9].

- *Amplitude condition*: The amplitudes for different subchannels have the same shape, *i.e.*,

$$|\Phi_k(f)|^2 = C + Q(f - f_k), \text{ for } |f - f_k| < \Delta f,$$

for $k = 0, 1, \cdots, N-1$, where $f_k = f_o + k\Delta f$ is the center frequency of the k-th subchannel. Furthermore, $Q(f)$ is a symmetric real function that is zero outside $[-\Delta f, \Delta f]$ and satisfies

$$Q(f) = Q(-f), \text{ for all } |f| \leq \Delta f,$$

and

$$Q(f) = -Q(\Delta f - f) \text{ for all } 0 \leq f \leq \Delta f,$$

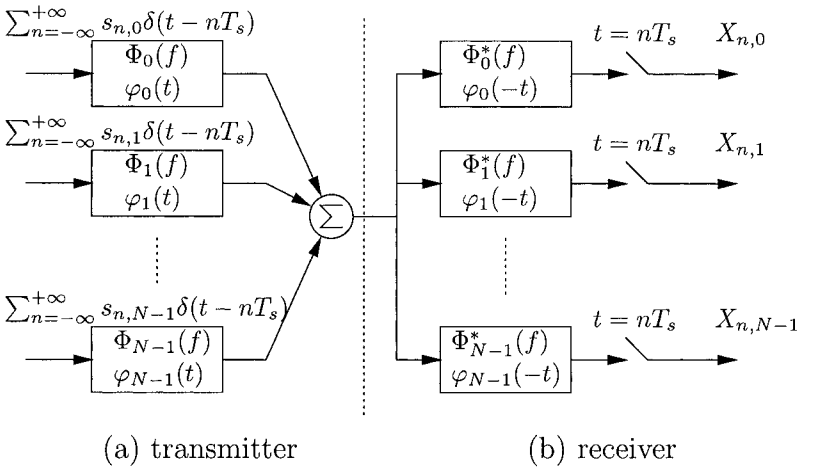

Figure 2.9. An orthogonal approach based band-limited multicarrier scheme.

and C in the above is a constant such that $C + Q(f)$ is nonnegative for $|f| \leq \Delta f$.

- *Phase condition*: The phases for different subchannels also have the same shape, *i.e.*,

$$\theta_k(f) = \theta(f - f_k), \text{ for } |f - f_k| < \Delta f.$$

The $\theta(f)$ in the above equation satisfies

$$\begin{aligned}\theta(f) &= m\pi\frac{f}{2\Delta f} + \alpha_0 + \sum_n \alpha_{2n+1}\cos\left((2n+1)\pi\frac{f}{\Delta f}\right) \\ &\quad + \sum_n \alpha_{2n}\sin(2n\pi\frac{f}{\Delta f}),\end{aligned}$$

where m is any odd integer and α_n's for all integer n's are arbitrary (real) numbers.

One of example in this category of multicarrier modulation is to choose

$$Q(f) = \frac{1}{2}\cos\left(\pi\frac{f}{\Delta f}\right),$$

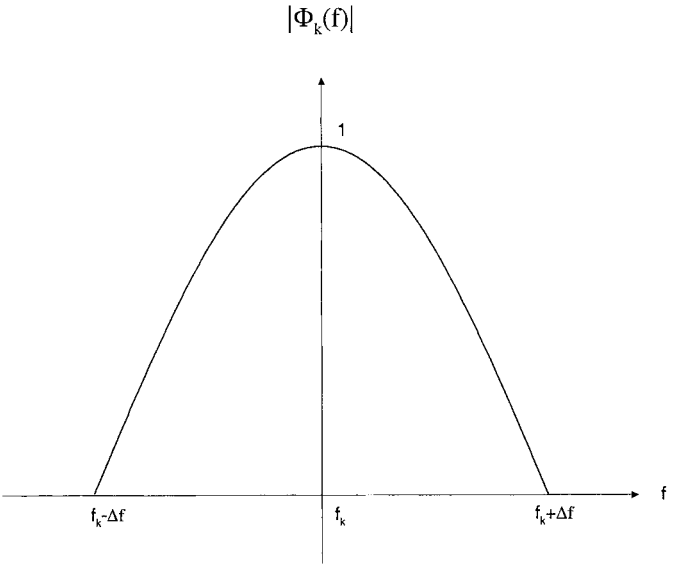

Figure 2.10. An example of amplitude shaping

and $C = 1/2$. Then

$$|\Phi_k(f)|^2 = \frac{1}{2} + \frac{1}{2}\cos\left(\pi\frac{f - f_k}{\Delta f}\right)$$

and

$$|\Phi_k(f)| = \cos(\pi\frac{f - f_k}{2\Delta f}),$$

which is shown in Figure 2.10

2.3.2 Filter Approach

Filter bank based multicarrier modulation was proposed by Saltzberg in [10]. The modulator and demodulator of this scheme are shown in Figure 2.11. All filters $F(f)$'s in the transmitter and receiver are identical and are assumed to be real. It is demonstrated in [10] that the use of the same filtering

at transmitter and receiver assures optimum performance for the AWGN channels. In order to eliminate the possibility of interference between any channels that are not immediately adjacent, the filters are bandlimited to the subchannel space, Δf, that is

$$F(f) = 0, \quad |f| \geq \Delta f,$$

and the transmit and receive filters in tandem have a Nyquist roll-off,

$$F^2(f) + F^2(\Delta f - f) = 1, \quad 0 \leq f \leq \Delta f. \tag{2.3.1}$$

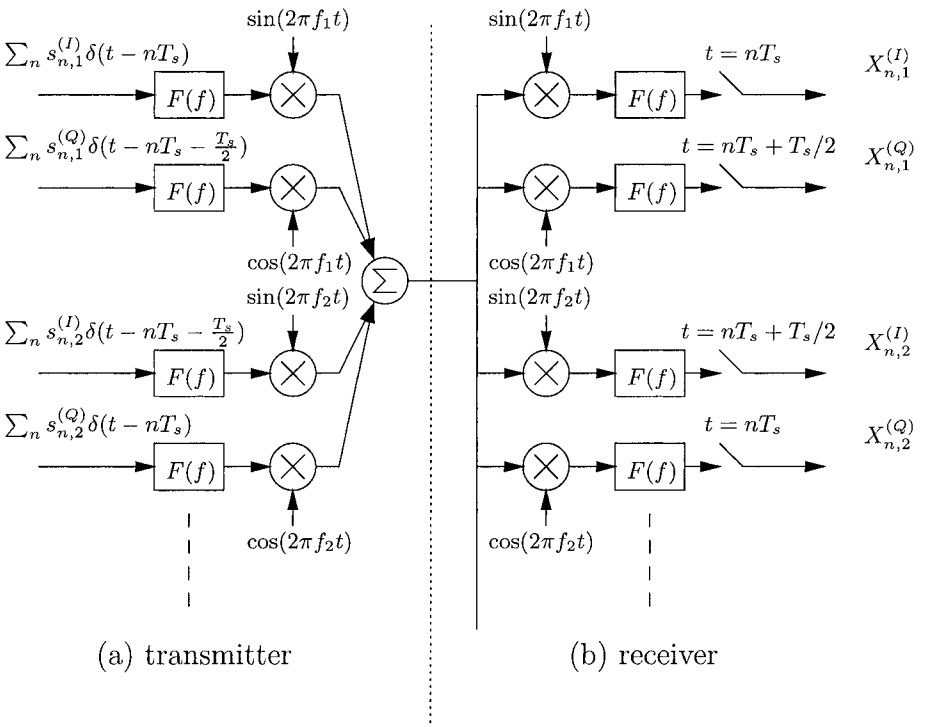

Figure 2.11. A filtering based multicarrier scheme.

The symbol duration for each stream is $T_s = 1/\Delta f$, and the timing of the two streams for the same subchannel are staggered by $T_s/2$. Adjacent

channels are staggered oppositely so that the data streams that modulate the cosine carriers of the even numbered channels and the sine carriers of the odd numbered channels are in phase. Consequently, the pass-band expression of the modulated signal from the transmitter is the following:

$$\begin{aligned} s(t) &= \sum_{k \text{ odd}} \sum_{n=-\infty}^{+\infty} s_{n,k}^{(I)} f(t - nT_s) \cos(2\pi f_k t) \\ &+ \sum_{k \text{ odd}} \sum_{n=-\infty}^{+\infty} s_{n,k}^{(Q)} f(t - nT_s - T_s/2) \sin(2\pi f_k t) \\ &+ \sum_{k \text{ even}} \sum_{n=-\infty}^{+\infty} s_{n,k}^{(I)} f(t - nT_s - T_s/2) \cos(2\pi f_k t) \\ &+ \sum_{k \text{ even}} \sum_{n=-\infty}^{+\infty} s_{n,k}^{(Q)} f(t - nT_s) \sin(2\pi f_k t), \end{aligned}$$

where $f(t)$ is the inverse Fourier transform of $F(f)$, $f_k = f_o + k\Delta f$, and $s_{n,k}^{(I)}$ and $s_{n,k}^{(Q)}$ are the information-bearing real random variables.

It can be shown that for the ideal channel (distortionless and noiseless), the demodulator can recover the transmitted sequences $a_{n,k}$ and $b_{n,k}$ without the ISI and ICI, if $F(f)$ satisfies (2.3.1).

For channels with linear distortion, the ISI and ICI are analyzed in [10]. The equalization for the filter based approach to reduce ISI and ICI is studied in [41].

2.3.3 General Multicarrier Modulation

We have discussed two special multicarrier modulations: time-limited form (OFDM) and band-limited form. Here we describe general multicarrier modulations.

To facilitate the basic concept of orthogonal multicarrier modulations, we first introduce *(T_s-shift) orthogonal complex functions.* A set of N complex functions, $\varphi_k(t)$ for $k = 0,\ 1, \cdots,\ N-1$, are called T_s-shift orthogonal if for any $k,\ l$ and $n,\ m$,

$$\int_{-\infty}^{+\infty} \varphi_k(t - nT_s)\varphi_l^*(t - mT_s)dt = c\delta[k - l]\delta[n - m], \tag{2.3.2}$$

where c is a positive constant. For simplicity, we may assume that the set is normalized, *i.e.* $c = 1$.

Based on a T_s-shift orthogonal complex function set, a general multicarrier transmitter and receiver can be designed. Let $s_{n,k}$ represent the information to be transmitted at the k-th subchannel of the n-th block. Then, the complex baseband signal transmitted over the channel can be expressed as

$$s(t) = \sum_{n=-\infty}^{+\infty} \sum_{k=0}^{N-1} s_{n,k}\varphi_k(t - nT_s). \tag{2.3.3}$$

In an AWGN channel, the received signal is

$$x(t) = s(t) + n(t), \tag{2.3.4}$$

where $n(t)$ is additive white complex Gaussian noise with zero mean and variance N_o. The transmitted sequence can be detected by

$$\begin{aligned} X_{n,k} &= \int_{-\infty}^{+\infty} x(t)\varphi_k^*(t - nT_s)dt \\ &= \int_{-\infty}^{+\infty} (s(t) + n(t))\varphi_k^*(t - nT_s).dt \end{aligned} \tag{2.3.5}$$

Because of the orthogonality of $\{\varphi_k(t - nT_s)\}$, (2.3.5) reduces to

$$X_{n,k} = s_{n,k} + N_{n,k}, \tag{2.3.6}$$

where

$$N_{n,k} = \int_{-\infty}^{+\infty} n(t)\varphi_k^*(t - nT_s)dt. \tag{2.3.7}$$

Since $\{\varphi_k(t-nT_s)\}$'s are orthonormal for different n's or k's, the noise $N_{n,k}$ is zero-mean and with variance N_o, and is uncorrelated (therefore independent) for different n's and k's.

OFDM introduced in Section 2.1 is clearly a special case when $\varphi_k(t) = \frac{1}{\sqrt{T_s}} e^{j\frac{2\pi kt}{T_s}}$.

http://www.springer.com/978-0-387-29095-9

Orthogonal Frequency Division Multiplexing for Wireless Communications

Li, Y.G.; Stuber, G.L. (Eds.)

2006, XII, 306 p., Hardcover
ISBN: 978-0-387-29095-9